Dynamics of Heterogeneous Azeotropic Distillation Columns

A new dynamic model has been developed for heterogeneous azeotropic distillation columns, which is capable of automatically detecting and accounting for multiple liquid phases on trays at each instant of time. Extensive dynamic simulations have been carried out for the heterogeneous distillation of ethanol, water and benzene. Our results are in general agreement with prior work, which shows that this class of separations can be expected to exhibit multiple steady states, complex dynamic behavior, and parametric sensitivity. One of the most unexpected results was that these systems exhibit parametric sensitivity with respect to small changes in column pressure. For systems vented to the atmosphere, small increases in the barometric pressure lead to loss of interface in the decanter over a 24-hour period. If small pressure variations of this sort are left uncontrolled long enough, the entire separation will fail. Small decreases in the barometric pressure do not have such a disastrous effect.

Maurizio Rovaglio
Dipartimento di Chimica Industriale
ed Ingegneria Chimica
G. Natta
Politecnico di Milano
20133 Milano, Italy

Michael F. Doherty
Department of Chemical Engineering
Goessmann Laboratory
University of Massachusetts
Amherst, MA 01003

Introduction

It is well known in the chemical industry that heterogeneous distillation is an economical technique for separating azeotropic mixtures. Unfortunately, it is also an exceptionally difficult process to operate and control. These columns are often observed to behave erratically or to suddenly lose product purity for no obvious reason. Over the last decade or so, these problems have sparked academic interest, and a number of important publications have emerged.

It is now widely reported in the literature that within certain ranges of column specifications, heterogeneous distillation columns exhibit multiple steady-state solutions. The first reported instance of this phenomenon was by Magnussen et al. (1979), who found that with identical column specifications and identical UNIQUAC interaction parameters (given by Gmehling and Onken, 1977a), three different sets of state variables (T_n, $\underline{x}_n$, $n = 1, \ldots N$) satisfied a constant molar overflow model for the ethanol-water-benzene distillation in a tower with 27 stages operating at 1-atm pressure (see Figure 1). This stimulated further research by Prokopakis and Seider (1983a, b) who used a more complete column model in which the energy balances and the decanter were included. They confirmed the presence of three quite different operating regimes with three different, but very similar, sets of specifications for the same column used by Magnussen et al. (1979) (although the UNIQUAC parameters used in the Prokopakis and Seider study were different than those used by Magnussen et al.). [In fact, there was an earlier study by Shewchuk (1974) who also found multiple steady-state solutions for the ethanol-water-benzene distillation with a column model that included the energy balances and the decanter. However, these results were never published.] More recent and quite detailed studies on this system by Venkataraman and Lucia (1988) confirm the presence of two regular turning points and three steady states over a narrow range of operating conditions. Figure 1 shows the comparison between the composition profiles obtained by Magnussen et al. (1979) and Prokopakis and Seider (1983a, b).

Multiple steady states have also been observed to occur for the dehydration of isopropanol with cyclohexane in a 38-tray tower (Prokopakis and Seider, 1983b), and for the dehydration of secondary butyl alcohol with disecondary butyl ether (Kovach and Seider, 1988) in a 41-tray tower. Kovach and Seider (1988) compare the simulation results with experimental data and conclude, "the presence of two solutions in such close proximity is consistent with the experimentally observed erratic behavior of the tower."

These studies demonstrate the very complex and highly sensitive response of heterogeneous distillation systems to changes in initial conditions, operating conditions, and model parameters. Moreover, recent work by Pham, Ryan, and Doherty (1989) shows that infinitesimal changes in some of the design variables lead to large variations in the steady-state composition and tem-

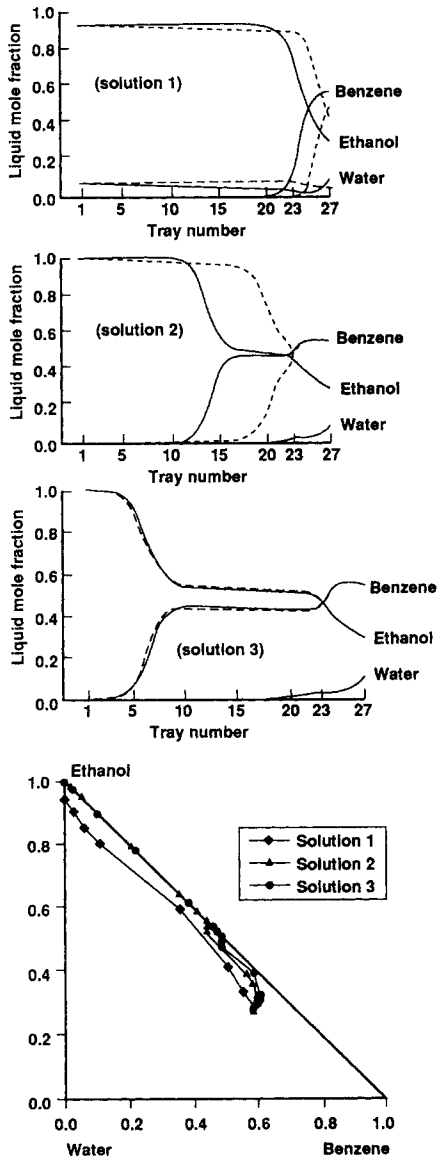

Figure 1. Three different steady-state composition profiles for the benzene-ethanol-water system obtained by Prokopakis and Seider (1983).

The dashed lines represent the result of Magnussen et al. (1979). For clarity, the profiles shown in the triangular diagram refer to the results of Prokopakis and Seider alone.

perature profiles in the column. For example, consider the distillation of isopropanol-water-benzene into a bottom stream containing 99.99 mol % isopropanol and an overall decanter composition that is constant and fixed. Changes in the bottom stream benzene mole fraction from 1×10^{-16} to 0.25×10^{-5} or to 0.75×10^{-4} lead to three completely different steady-state composition profiles in columns with three quite different designs, requiring 32, 15 and 17 theoretical trays, respectively. This phenomenon could be easily mistaken for the existence of several very different designs with identical bottom and decanter compositions, but with completely different steady-state column composition profiles.

All these observations suggest that great care should be taken in the choice of operating conditions for these columns and that further studies on the dynamics, stability, operability and control of these complex systems would be worthwhile. This paper is motivated by these problems.

Previous dynamic models have also one essential feature missing, namely, the ability to incorporate multiple liquid phases on the trays during the time evolution. Since heterogeneous distillation exploits the presence of liquid-liquid immiscibilities, this has been a serious deficiency in previous algorithms and simulations. This has motivated us to build a dynamic model which is capable of detecting and accounting for the presence of multiple liquid phases at each instant in time without specifying the location of the heterogeneous trays. The heterogeneous distillation of ethanol and water using benzene as entrainer was studied extensively so as to compare our results with all the previous results reported in the literature. In addition, we report some new results on the parametric sensitivity of these systems. Of particular interest is the high sensitivity of the system to very small changes in column pressure. For systems vented to the atmosphere, small increases in the barometric pressure lead to the loss of interface in the decanter over a period of 24 hours, while small decreases in the barometric pressure do not have such disastrous effects.

Mathematical Models

Following the equation structure presented in a previous paper (Rovaglio et al., 1986), we have constructed a dynamic model for heterogeneous azeotropic systems, which describes the behavior of all the principal state variables throughout the column. A schematic representation of a typical plate is shown in Figure 2. Each stage is allowed to have a liquid and vapor sidestream, one feed, one thermal duty, and two possible liquid phases. The column has N vapor-liquid theoretical trays numbered from the reboiler (stage 1) up to the top tray of the column (stage N), plus one liquid-liquid equilibrium stage (condenser-decanter system, numbered as stage $N + 1$). In formulating such a model, the following simplifications have been made:

a. Capacitance terms due to the downcomer are neglected.
b. Vapor holdup over the plate is neglected.
c. Liquid and vapor phases are mixed well.
d. The liquid and vapor streams leaving each stage are in phase equilibrium.

If there are C components in the column, then the following $(C + 5)$ equations can be written for each stage:

C Material Balances

$$\frac{dM^o_{i,n}}{dt} = L_{n+1}x^o_{i,n+1} - (L_n + U_n)x^o_{i,n} - (V_n + W_n)y_{i,n} + V_{n-1}y_{i,n-1} + F_{i,n} \quad i = 1, \ldots, C \quad (1)$$

1 Energy Balance

$$\frac{dE_n}{dt} = V_{n-1}H^V_{n-1} - (L_n + U_n)H^L_n - (V_n + W_n)H^V_n + L_{n+1}H^L_{n+1} + F_nH^F_n + Q_n \quad (2)$$

2 Fluid Dynamic Relationships

$$\sum_{i=1}^{C} M^o_{i,n} = M^*_n - \tau^V(V_n + W_n) + \tau^L(L_n + U_n) \quad (3)$$

$$P_n = P_{n+1} + \Delta P_{n+1}(L_n, V_n, U_n, W_n, \text{geometry}) \quad (4)$$

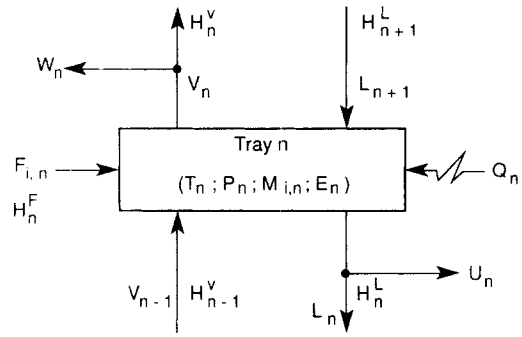

Figure 2. A schematic representation of tray *n*.

1 Vapor-Liquid Equilibrium Equation

$$\sum_{i=1}^{C} K_{i,n}(T_n, P_n, \underline{x}_n^o)x_{i,n}^o = 1 \tag{5}$$

1 Definition of the Total Energy per Plate

The total energy per plate should actually be the total internal energy per plate (Luyben, 1973; Stephanopoulos, 1984). However, we follow the common practice of approximating it by the total enthalpy per plate (Gallun and Holland, 1980; Boston et al., 1981; Prokopakis and Seider, 1983b).

$$E_n = H_n^L \sum_{i=1}^{C} M_{i,n}^o \tag{6}$$

where $x_{i,n}^o$ is the overall liquid composition of component i on tray n, defined by $x_{i,n}^o = M_{i,n}^o / \Sigma_{i=1}^{C} M_{i,n}^o$. This constitutes an algebraic and differential system of equations that can be solved using a global approach (Gallun and Holland, 1980). At each time step, we can obtain the following state variables for every tray: temperature (T_n), pressure (P_n), total energy (E_n), total molar holdup of each component ($M_{i,n}^o$), and the liquid (L_n) and vapor (V_n) flow rates leaving the stage.

Equations 3 and 4 reflect the level of fluid dynamic simplification used in the model. Equation 3, in particular, defines a linear relationship between the total liquid holdup and the liquid and vapor flow rates leaving the stage. The constants M_n^*, τ_n^V, τ_n^L depend on the particular type of plate (sieve, bubble caps, etc.) and on the geometric characteristics of the column. The definition of the pressure profile in the column, Eq. 4, needs the evaluation of pressure drops across the tray. Values for the quantities M_n^*, τ_n^L, τ_n^V, $\Delta P_{n+1}(V_n, L_n, W_n, U_n,$ geometry) are calculated from correlations available in the literature; see, for example, Treybal (1980) or, for an extensive treatment, Glitsch (1974) and Nutter (1976).

Phase Equilibrium Calculations

Equation 5 needs to be discussed in a little more detail since the thermodynamics of the system can influence the structure of the algorithm. When only one liquid phase exists on the tray and when the vapor can be considered ideal, the system (Eqs. 1–6) is self-consistent and the vapor composition can be simply and explicitly defined as a function of temperature, pressure and liquid composition:

$$y_{i,n} = K_{i,n}(T_n, P_n, x_{i,n}^o)x_{i,n}^o \quad i = 1, \ldots, C \tag{7}$$

No inner iteration loops are required to calculate $\underline{y}$, and Eq. 7 can be directly substituted in the previous system of Eqs. 1–6. The situation changes when a liquid-phase split occurs on the tray. In this case, liquid-liquid-vapor calculations must be included in the model. For this purpose, Eq. 5 of the main system (Eqs. 1–6), must be replaced by the following subset of equations:

$$x_{i,n}^o = \alpha_n x_{i,n}^1 + (1 - \alpha_n)x_{i,n}^2 \quad i = 1, \ldots, C \tag{8}$$

$$\gamma_{i,n}^1(T_n, \underline{x}_n^1)x_{i,n}^1 = \gamma_{i,n}^2(T_n, \underline{x}_n^2)x_{i,n}^2 \quad i = 1, \ldots, C \tag{9}$$

$$\sum_{i=1}^{C} x_{i,n}^1 - \sum_{i=1}^{C} x_{i,n}^2 = 0 \tag{10}$$

$$y_{i,n} = K_{i,n}(\underline{x}_n^1, T_n, P_n)x_{i,n}^1 \quad i = 1, \ldots, C \tag{11}$$

which are solved as a procedure. That is, Eqs. 8 to 11 are solved as a separate block at each function evaluation. Superscripts 1 and 2 represent the two immiscible liquid phases, and α_n is the molar ratio between the amount of phase 1 and the total liquid phase on tray n.

The system of Eqs. 8–11 constitutes an isothermal vapor-liquid-liquid flash problem which can be solved to find α_n, the vapor and liquid compositions $\underline{y}_n$, $\underline{x}_n^1$, $\underline{x}_n^2$, knowing the temperature, pressure and overall liquid composition. All these variables (T_n, P_n, $M_{i,n}^o$, hence $x_{i,n}^o$) are known at each function evaluation point through the integration of the main system of Eqs. 1–6. Equations 9 and 10 are strongly nonlinear and numerically-sensitive. Moreover, Eq. 9 admits the trivial solution $x_{i,n}^1 = x_{i,n}^2 = x_{i,n}^o$ for $i = 1, \ldots, C$. This requires a careful choice of the algorithm adopted to solve the LLVE subproblem. On the one hand, it is important to avoid unwanted solutions. On the other hand, the computing time must be kept to a reasonable level and convergence accelerators are strongly recommended. An extensive discussion about the features and the solution of such a system is beyond the scope of this paper; more information and further details can be found in Prausnitz et al. (1980), whose approach has been adopted here.

The solution of the complex system of Eqs. 8–11, instead of the simple equation (Eq. 7), is activated only when the presence of the two liquid phases is detected on the tray. Thus, in order to decide when to switch the equilibrium calculation, we included in our model a stability test which avoids unwarranted computational efforts and defines the thermodynamic state for every tray at each function evaluation point. The test works by using a spline fit of the liquid-liquid-vapor envelope in order to check whether the overall liquid composition lies inside or outside the absolutely stable liquid-phase region (see Ryan, 1989). This solution procedure allows us to rapidly check for phase splitting throughout the column and for all simulation time, without assigning "*a priori*" the trays where the phenomenon might occur, without reducing the robustness of the model itself. These features distinguish this model from those of Magnussen et al. (1979) and Prokopakis and Seider (1983a,b) which were not able to predict or accomodate multiple liquid phases on the trays inside the column at each iteration step (for steady-state simulations) or as a function of time (for dynamic simulations). This additional feature to the algorithm allows us to study effects which could not be studied with previous dynamic models, e.g., impact of liquid-phase splitting along the column or the pres-

ence of multiple steady-state solutions or dynamic loss of interface in the decanter.

Reboiler and Condenser-Decanter

Relations 1–11 can be applied to all the stages inside the column; however, the reboiler and the condenser require further specifications.

For the reboiler, Eq. 3 was replaced by the Francis weir formula, which is a nonlinear fluid dynamic relationship and allows us to calculate the liquid flow rate (L_1) leaving the reboiler. Otherwise, the equations remain unchanged. For more details, see Rovaglio et al. (1986).

The last stage consists of the system condenser plus decanter as shown in Figure 3. In the formulation of such a submodel, the following characteristics have been assumed:

a. Subcooled total condenser is used.

b. The decanter and condenser are at the same temperature and pressure, which are given assigned values. The system is assumed to be vented to the atmosphere, thus the assigned pressure is the barometric pressure.

c. Liquid-liquid equilibrium conditions exist in the decanter. The equations that we need for this model are exactly the same equations defined before or, at least, they follow the same structure previously reported. Very few modifications must be introduced. In particular, Eq. 3, which describes the fluid dynamic behavior and allows us to compute the liquid flow rate leaving the tray, can be replaced by the following relations derived from Bernoulli's equation (see Figure 3):

$$h_1 + h_2 - h_3 = \frac{v_1^2}{2g} = \left(\frac{L_{N+1}^1}{c_{N+1}^1 0.61\, s_d^1}\right)^2 / 2g \qquad (3a)$$

$$h_1\rho^1/\rho^2 + h_2 = \frac{v_2^2}{2g} = \left(\frac{L_{N+1}^2}{c_{N+1}^2 0.61\, s_d^2}\right)^2 / 2g \qquad (3b)$$

where c_{N+1}^1 and c_{N+1}^2 are the molar concentrations in the two phases; ρ^1 and ρ^2 are the mass densities; s_d^1 and s_d^2 are the downcomer cross-sectional areas; and the factor 0.61 represents a reasonable estimate for the discharge coefficient (see Perry, Chilton, and Kirkpatrick, 1969, pp. 5-5 and 5-11). With these two correlations we can evaluate the two liquid flow rates leaving the decanter (L_{N+1}^1, L_{N+1}^2). The heights h_1 and h_2, which appear in Eqs. 3a and 3b, can be deduced by the individual molar holdups present in the decanter:

$$h_1 = \frac{\alpha_{N+1} \sum_{i=1}^{C} M_{i,N+1}^o}{c_{N+1}^1 \pi D_d^2/4}$$

$$h_2 = \frac{(1 - \alpha_{N+1}) \sum_{i=1}^{C} M_{i,N+1}^o}{c_{N+1}^2 \pi D_d^2/4}$$

where D_d is the decanter diameter.

As mentioned above, the condenser is a total subcooled condenser which implies that no vapor flow rate leaves the stage; hence, no pressure drop occurs across the vent valve. Therefore, Eqs. 4 and 11 can be disregarded in the formulation of this submodel.

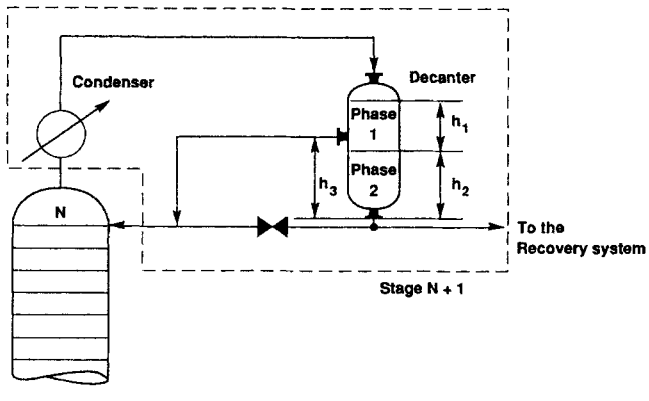

Figure 3. A schematic representation of state $N + 1$.

Algorithm

The overall dynamic model consists of $(C + 1)N$ differential equations and $4N$ algebraic equations, plus $(3C + 1)N^*$ algebraic equations arising from the phase split on N^* stages. Regardless of whether or not two liquid phases are present on some of the trays, the model needs $(C + 1)N$ initial conditions. We have taken these initial conditions to be the steady-state conditions of the column for a given set of input variables consistent with the degrees of freedom. For this purpose, we have used a Wang Henke method, modified in such a way as to take into consideration the vertical pressure profile and, if needed, the LLVE calculations as already reported by Buzzi Ferraris and Morbidelli (1981). The boiling point method, mentioned in the latter work, was improved in order to define where and when LVE and LLVE must be taken into account and, at the same time, avoiding explicit preassignments of multiphase tray locations. The modified Wang-Henke solution procedure obtained has the same advantages and limits that are well known for the original two-phase boiling point method. This method, however, requires a small amount of computation time and usually provides a steady-state solution even when the starting point is poor. From the resulting steady-state solution, all the initial conditions that we need for the dynamic model can be consistently defined.

Due to the intrinsic nature of distillation columns, the time constant spectrum is very wide (e.g., stiffness ratios of 10^6 or greater). Therefore, both for the presence of algebraic equations and for the stiffness of the differential equation, the use of a completely implicit integration method (such as Gear's method) is strongly recommended (Ranzi et al., 1986). Our program uses a modified version of the LSODES package which is a solver for ordinary differential equations with general sparse Jacobian matrices (Hindmarsh, 1983). Our modified version has extended the original program so that algebraic-differential systems can also be handled (Feng et al., 1984). This package uses the Yale code for nonsymmetric sparse matrices (Eisenstatt et al., 1977) and backward differentiation (Gear, 1971) for the numerical integration of the system. More details from a numerical point of view can be found in Ranzi et al. (1985, 1986).

When the liquid-phase split is detected on a tray by the stability test, the resulting $(3C + 1)$ algebraic equations (Eqs. 8–11) can be solved separately for each such stage and at each time. The decoupling of this subset of equations from the main system can result in an increase of computing time, but allows us to fol-

low the behavior of the column without specifying beforehand where the LLVE should be present. To the best of our knowledge, this is the first dynamic model reported in the literature that can do such calculations.

Simulation Results

All the numerical examples considered in this article refer to a 27-tray column (including the reboiler) and condenser to dehydrate a stream containing 89×10^{-3} kmol/min of ethanol and 11×10^{-3} kmol/min of water. This feed is a saturated liquid introduced on stage 23. The entrainer is benzene. The geometric characteristics and the dimensions of the auxiliary equipment are reported briefly in Table 1. This example was already reported and studied by Magnussen et al. in 1979 and later by Prokopakis and Seider (1983a,b), and Venkataraman and Lucia (1988). The following presentation of our simulation results will be related to these previous articles.

Comparison with Magnussen et al.

As mentioned previously, Magnussen et al.'s paper does not include the decanter model and substitutes the reflux stream from the condenser with a second feed, fixed in composition, temperature, and flow rate. Moreover, their model assumes that the liquid phase on the trays is everywhere homogeneous at all the iteration steps. To test our computer code, we initially simulated the system described by Magnussen et al. (1979), using identical model parameters, column design, operating conditions, and with the condenser/decanter system omitted. The reflux stream was kept at the same constant temperature, composition, and flow rate reported in their paper. Our results were in agreement with those obtained by Magnussen et al.

We now report new results. In order to understand the possible feedback effects of the entrainer-rich-phase reflux stream, we modified the original structure by introducing the heterogeneous decanter model in the top of the column (as suggested by Prokopakis and Seider, 1983a). All results reported in this section are with specific reference to this modified column. Figure 4 gives a comparison between the original and modified piping layout. The light phase leaving the condenser is completely recycled to the column while the heavy phase constitutes the top product. The condenser bypass, shown in Figure 4, provides the

Table 1. Main Geometric Characteristics of the Azeotropic Column Used in All the Reported Examples

Tray Layout	
26 sieve trays	
Tower diameter	0.6986 m
Tray spacing	0.5000 m
Hole diameter	0.0050 m
Pitch	0.0150 m
Active area	0.2300 m^2
Kettle Reboiler Geometry	
Free volume	0.9000 m^3
Diameter	1.2000 m
Length	2.0000 m
Decanter Geometry	
Diameter	0.5000 m
Length	2.0000 m
h_3 (see Figure 3)	1.0000 m

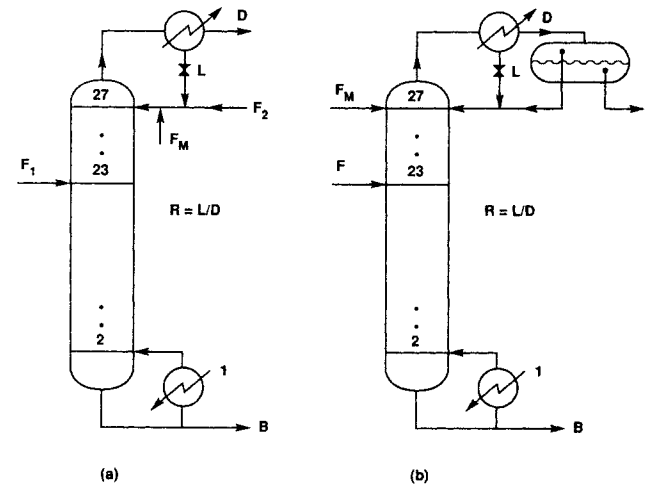

Figure 4. Main azeotropic distillation column: configuration and reflux ratio definition adopted. *(a) Magnussen et al. (1979) and (b) the present work.*

required degree of freedom for column operability (i.e., provides a method of adjusting the reflux flow).

All the calculations presented were performed assuming ideal behavior for the vapor phase and vapor pressures computed using the Antoine equation with coefficients given by Gmehling and Onken (1977a). Furthermore, in this first section, the liquid-phase activity coefficients were modeled using the modified UNIQUAC equation with binary parameters given by Gmehling and Onken (1977a) for liquid-vapor and liquid-liquid-vapor equilibrium on the trays, and interaction parameters reported by Prausnitz et al. (1980) for liquid-liquid equilibrium calculations in the decanter (which are calculated from both binary and ternary data). All the cited parameters are reported in Prokopakis and Seider (1983a). These thermodynamic parameters are as close to those used by Magnussen et al. as is possible to achieve with the decanter included in the column model. The Gmehling and Onken parameters cannot be used for the liquid-liquid equilibrium calculations in the decanter because they give qualitatively incorrect phase behavior as described by Prokopakis and Seider (1983a). None of the previous studies which have extended the Magnussen et al. column to include the decanter have used such a faithful approximation to the Magnussen et al. thermodynamics.

The three degrees of freedom for the column were satisfied by assigning the reflux ratio (defined in Figure 4), the distillate flow rate, and the temperature of the total subcooled condenser as $R = 5.47$, $D = 87.6 \times 10^{-3}$ kmol/min, and $T_{N+1} = 298$ K, respectively. The entrainer make-up is fed to the top of the column and defined as $F_m = 1.5 \times 10^{-3}$ kmol/min. Note that all these specifications are the same as those used by Magnussen et al. (1979), with the exception of the flow rate D. When the condenser/decanter loop is closed, as in our simulations, the flows L and D in Figure 4a differ from flows L and D in Figure 4b even though their ratio is the same. It is not possible to make all the stream flows and compositions at the top of the column in Figure 4a identical to those in Figure 4b.

With these operating conditions, using the steady-state solver mentioned in the previous section, we found the composition profiles shown in Figure 5a. This solution defines the starting point for the dynamic solver. Using this approach, we imposed a

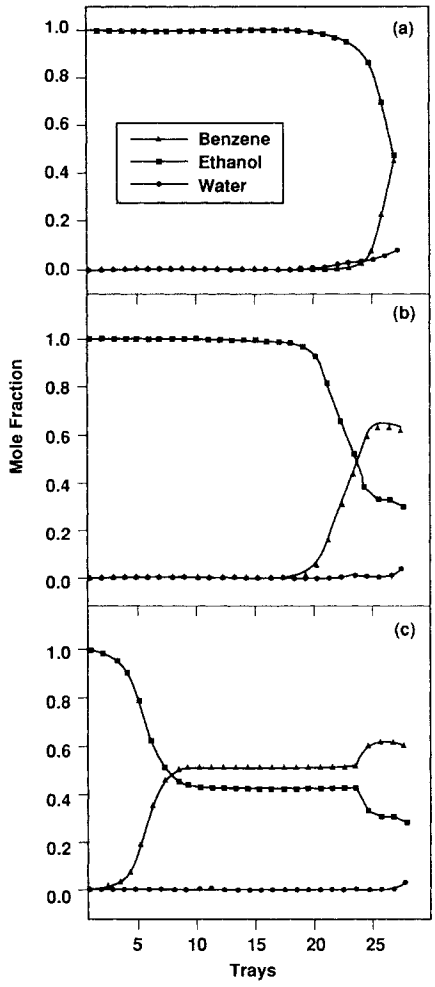

Figure 5. Three different steady-state solutions for the benzene-ethanol-water system obtained with the same column specifications and Gmehling-Onken's parameters for LVE and LLVE calculations.

ramp disturbance after 100 minutes by increasing the feed flow rate 10% in 1 minute. After 400 minutes of response time, an inverse disturbance returned the operating conditions to their original values. Following the transient behavior of the system, the column appears to "settle down" to the steady state reported in Figure 5b. This steady state, however, is unstable; and, continuing the dynamic simulation, we find that the composition profiles ultimately settle down to those given in Figure 5c. This last profile corresponds to the normal azeotropic distillation case where the high benzene composition is sustained far down the column, driving water to the top. In the profile reported in Figure 5a, the benzene composition drops rapidly in the rectifying section, hence a small amount of water can be found in the stripping section. The situation presented in Figure 5b is an intermediate between the first two. Figure 5c has the unusual feature that the ethanol and benzene profiles in the middle of the column, where water is essentially absent, cross the experimental composition of the ethanol-benzene binary azeotrope (ethanol ~55 mol %, benzene ~45 mol %). While this is true, the important point to note is that the profiles *do not* cross the model predicted composition of the ethanol-benzene binary azeotrope which contains ~38 mol % ethanol and ~62 mol % benzene. Thus, the thermodynamic model does not represent the real phase equilibria for this mixture very accurately as is seen in Figure 6a, and as is discussed in more detail later in this section.

Figure 7 summarizes the previous behavior of the column by showing the transient response of selected variables on tray 18. This figure clearly shows the shift from the first steady state to the third by way of the second. Thus, from these results, we can identify three different steady-state conditions, which correspond to the same column specification.

For the dynamic simulation, the three operating degrees of freedom were taken to be the reflux ratio, the reboiler and condenser heat loads instead of the distillate flow rate, the reflux ratio and the temperature of the subcooled condenser, which were used for the initial steady-state calculations. These new degrees of freedom for the dynamic simulation are more closely related to the actual manipulated variables available in the plant. When no disturbances are acting, however, the two sets of specifications are equivalent as shown in Figure 8. This figure presents the dynamic response of selected state variables in two different situations. The curve (i) is the response to a ramp vari-

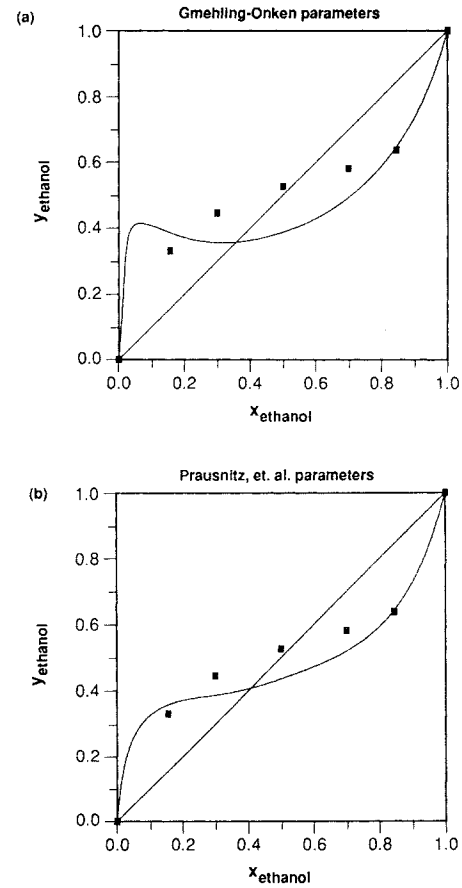

Figure 6. Equilibrium y-x diagrams for the mixture ethanol-benzene at 1-atm pressure, calculated using the UNIQUAC model. *(a) Gmehling and Onken interaction parameters and (b) Prausnitz et al. interaction parameters.*

The solid squares represent experimental data points taken from Gmehling and Onken (1977b, p. 411).

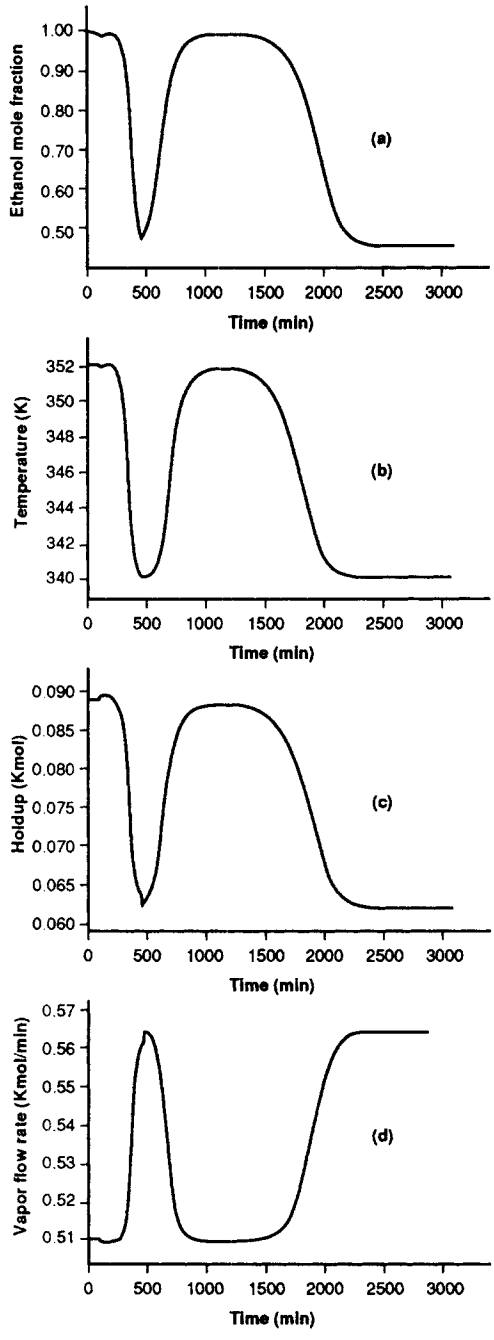

Figure 7. (a) Ethanol mole fraction; (b) temperature (K); (c) holdup (kmol); and (d) vapor flow rate (kmol/min) vs. time (min) on tray 18.

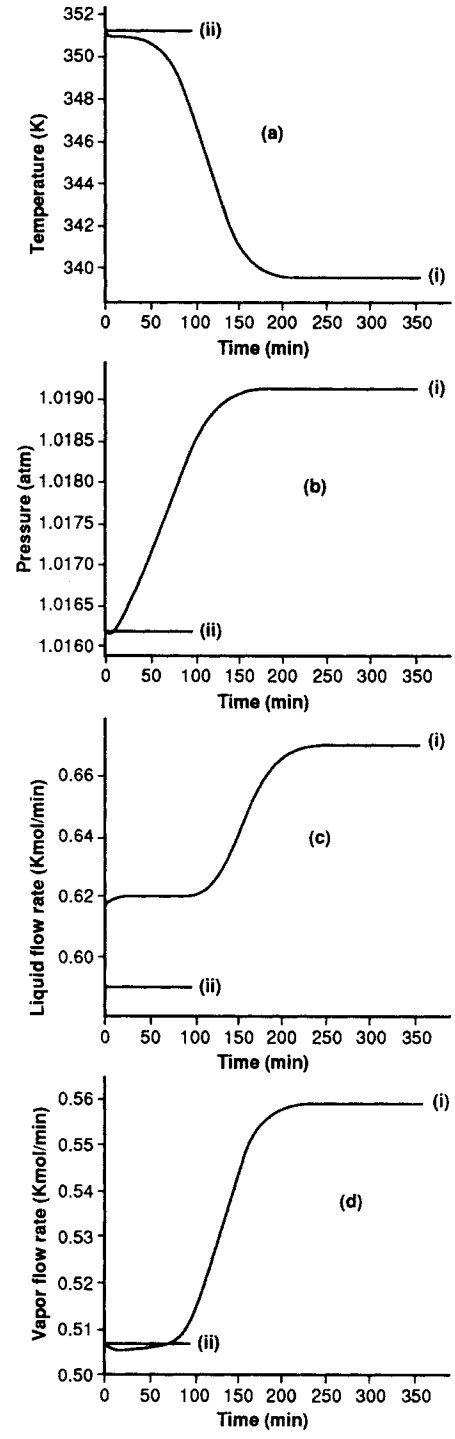

Figure 8. (a) Temperature (K); (b) pressure (atm); (c) liquid flow rate (kmol/min); and (d) vapor flow rate (kmol/min) vs. time (min) on tray 22.

(i) For a ramp increase of 10% in the feed flow rate over the course of one minute, beginning at time zero. (ii) No disturbance.

ation of 10% in the feed flow rate in 1 minute from the beginning. Curve (ii) is the response of the system when no disturbances are acting. The comparison shows that the first steady-state conditions (from the steady-state solver) are perfectly stable and that no numerical drift occurs as a result of introducing the dynamic solver and the change of specification variables.

Following these results, calculations were also performed using different values for the reflux ratio, and the corresponding multiplicity region observed is reported in Figure 9. This figure shows the ethanol mole fraction on the feed tray vs. the reflux ratio and displays the well-known "s" shape. This specific variable has been chosen because it has a large variation and gives rise to a clear bifurcation diagram. Also note the large range of reflux ratios where different steady-state solutions can be found.

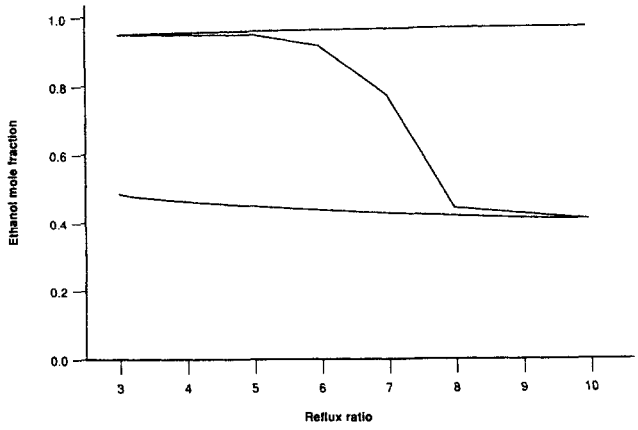

Figure 9. Mole fraction of ethanol on tray 23 (feed tray) vs. different values of the reflux ratio as defined in Figure 5.

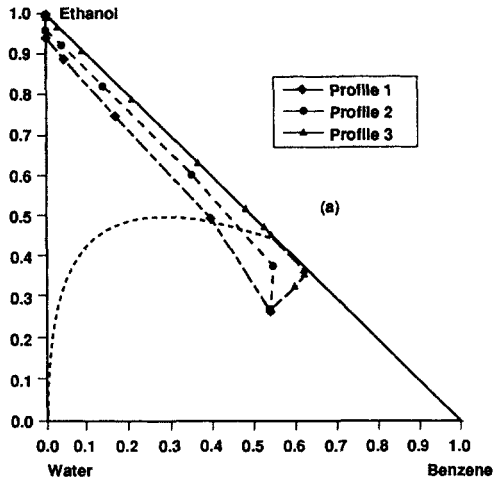

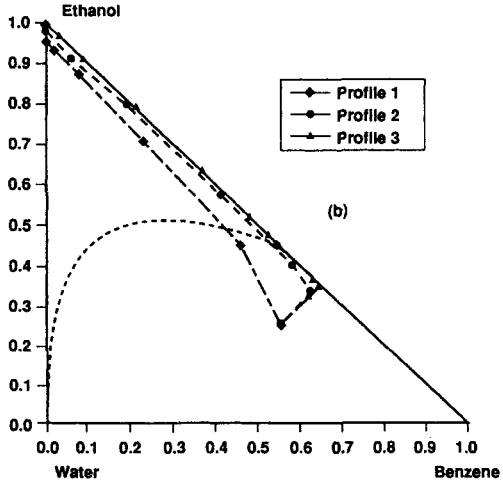

Figure 10. Three different steady-state composition profiles reported in Figures 6a, 6b and 6c, superimposed on the liquid-liquid-vapor envelope.

Both sets of calculations were carried out using Gmehling-Onken's parameters: (a) with LLVE calculations on the trays; (b) without LLVE calculations on the trays.

The presence of two regular turning points is consistent with the results reported by Venkataraman and Lucia (1988), who studied the same column but with different thermodynamic parameters for liquid-vapor calculations (given by Prausnitz et al., 1980).

Let us now analyze these results from a thermodynamic point of view. If we plot the three different solutions previously reported in Figure 5 together with the projection of the liquid-liquid-vapor envelope (Ryan, 1989) on the composition triangle diagram, we can see that some trays lie inside the heterogeneous region. As shown in Figure 10a, the composition profile 3, which corresponds to that reported in Figure 5c, has about 60% of the trays with two liquid phases. Magnussen et al. found no liquid-liquid split anywhere in the column for all the different steady states. However, more recently Baden and Michelsen (1987), working with the same column but with a different thermodynamic model (UNIFAC), confirm the presence of liquid-phase splitting in over 50% of the column trays (from 9 to 25). We repeated the calculations with the liquid-phase stability test turned off for the trays but not for the decanter and found the composition profiles reported in Figure 10b. The shape and the location of these profiles are very similar to the previous ones, and there are still trays located in the heterogeneous region (although, by decree, the simulator is unaware of it for these runs). Thus, the presence of multiple steady states and the basic shape of the steady-state composition profiles remain intact regardless of whether or not the liquid-phase heterogeneities are accounted for correctly.

From Figures 6a, 10a and 10b, we also note the poor agreement between the thermodynamic representation of the mixture using the UNIQUAC equation with the Gmehling and Onken parameters and the experimental data (see Bancroft and Hubard, 1942; Norman, 1945; Gmehling and Onken, 1977b, p. 411). From these papers, we know that the system water-ethanol-benzene is a type-1 system and does not exhibit immiscibility on two sides of the composition diagram. Prokopakis and Seider (1983a) have already reported this erroneous behavior

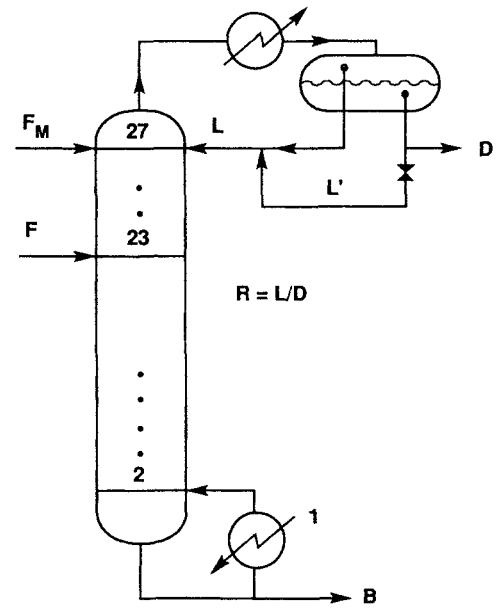

Figure 11. Alternative lay-out and reflux ratio definition.

predicted by the Gmehling and Onken parameters. They confined their study to the parameters reported by Prausnitz et al. (1980), which give a much better representation of the phase equilibrium (Ryan and Doherty, 1989). Figures 6a and 6b show the equilibrium y-x diagrams for a binary mixture of ethanol and benzene predicted from the UNIQUAC model using the Gmehling and Onken parameters (Figure 6a) and the Prausnitz et al. parameters (Figure 6b). Experimental data are also reported on these figures. Thermodynamic phase-stability theory requires $(\partial y/\partial x)_p > 0$ for a stable liquid phase. Therefore, the Gmehling and Onken parameters predict a region of liquid-liquid immiscibility and a *heterogeneous* binary azeotrope (of composition ~38 mol % ethanol and 62 mol % benzene) in this binary mixture. The data clearly show that no such immiscibility exists and that the azeotrope is a homogeneous azeotrope with composition ~55 mol % ethanol.

From now on, we too confine our study to these parameters at every point in the system. This set of parameters for the modified UNIQUAC equation is reported in Prokopakis and Seider (1982a).

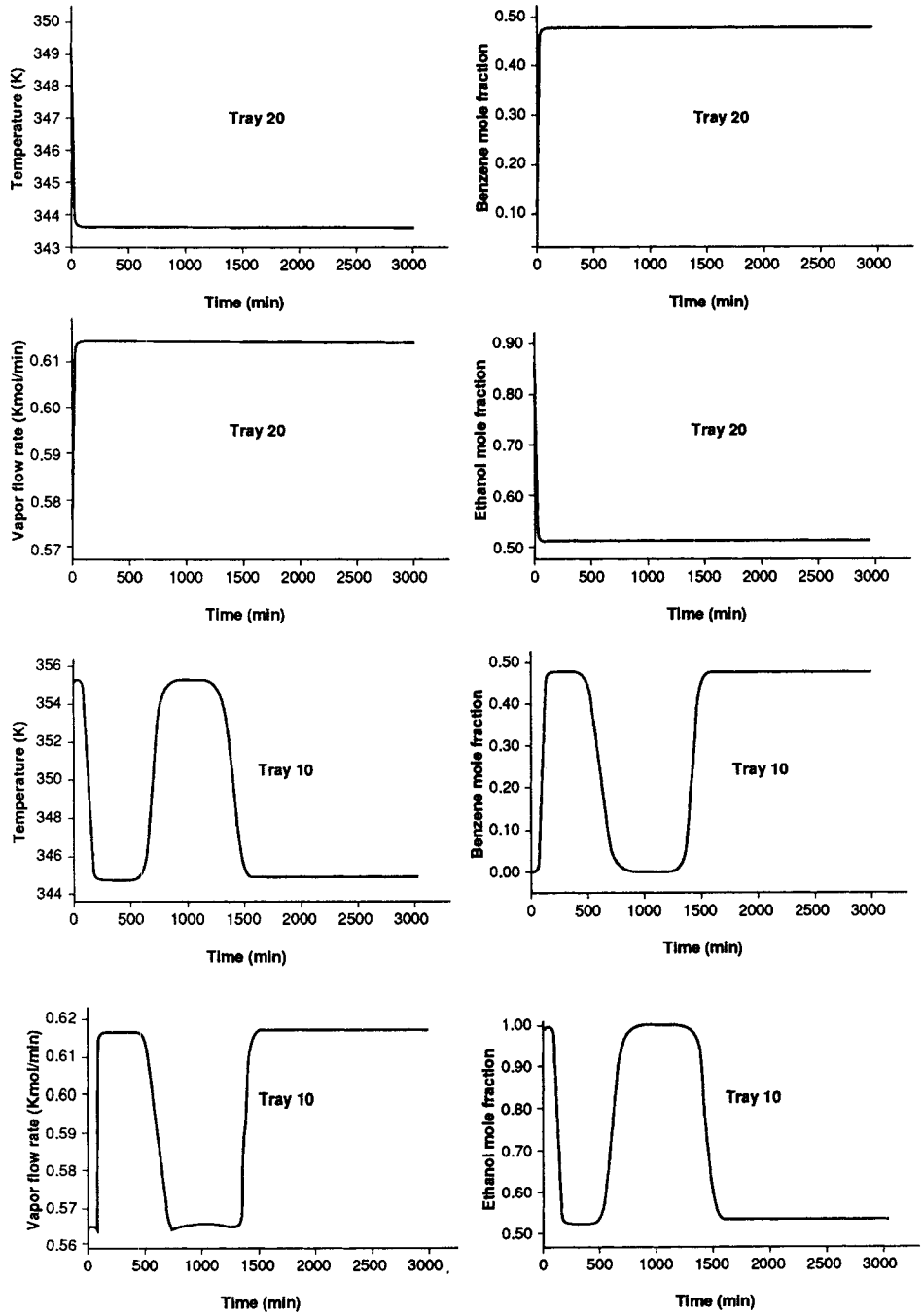

Figure 12. Temperature (K), benzene mole fraction, vapor flow rate (kmol/min), and ethanol mole fraction vs. time (min) on trays 10 and 20.

No disturbances are imposed on the system.

Comparison with Prokopakis and Seider

We begin by modifying the piping layout, abolishing the decanter bypass and introducing a partial recycle of the heavy phase leaving the decanter. This representation, reported in Figure 11, is very similar to the previous one (Figure 5b), but is preferred in practice for control purposes. Prokopakis and Seider (1983b) made this modification in their second paper, and we follow suit. All the geometric characteristics and operating conditions mentioned above remain exactly the same. With reference to Figure 11, the column specifications for the steady-state solver were defined as $R = 23.78$, $D = 21.378 \times 10^{-3}$ kmol/min and the same temperature was assigned to the subcooled condenser, $T_{N+1} = 298$ K. The entrainer make-up was fixed at $F_m = 1.962 \times 10^{-3}$ kmol/min.

With the Prausnitz et al. parameters, severe convergence problems were encountered while attempting to determine the steady-state solution for the column. It is difficult to tell whether the resulting solution from the steady-state solver is a real (unstable) steady state, because it was not possible to make the maximum residual of all the material balances arbitrarily small during the iteration steps. Instead, it asymptoted to about 10^{-5}, whereas, for the previous model parameters by Gmehling and Onken, typical values of the same residual were 10^{-6} or smaller. In any case, when this approximate solution is used to initialize the dynamic model, the state variables immediately drift away from their initial values.

Figure 12 summarizes the transient behavior of the column during the response time needed to achieve the stable solution. The variables reported in this figure show that two qualitatively different types of transient behavior occur in the same column section. As a matter of fact, all the variables reported for tray 20 reach the solution very rapidly, while the variables for tray 10 show a sort of "oscillating" behavior in the course of their transient towards a stable solution. Along the time coordinate, three different stationary points (the residuals of all the algebraic and differential equations are less than 10^{-4}) can be pointed out, namely, around 300 minutes, around 1,000, and after 1,500 minutes.

The three corresponding composition profiles are reported in Figure 13a, 13b and 13c, respectively. Using the corresponding composition, temperature and flow rate profiles as initial points for the steady-state solver, it is possible to confirm that they satisfy the convergence check (maximum absolute error on the material balances for every component and every tray $<10^{-6}$); consequently, they can be treated as three different steady-state solutions since they refer to the same column specifications. In other words, in this case, the dynamic solver becomes something like a continuation method and allows us to detect different stationary points. The results presented here are perfectly consistent with the corresponding ones presented by Venkataraman and Lucia (1988).

In Figure 14, these three steady-state profiles are superimposed on the liquid-liquid-vapor envelope, which was also calcu-

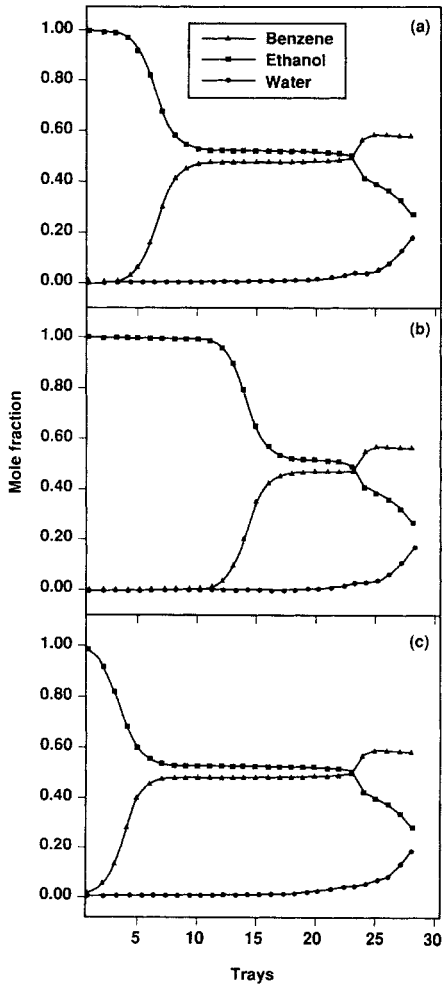

Figure 13. Three different steady-state composition profiles for the benzene-ethanol-water system obtained with same column specification and Prausnitz et al.'s parameters for LVE and LLVE calculations.

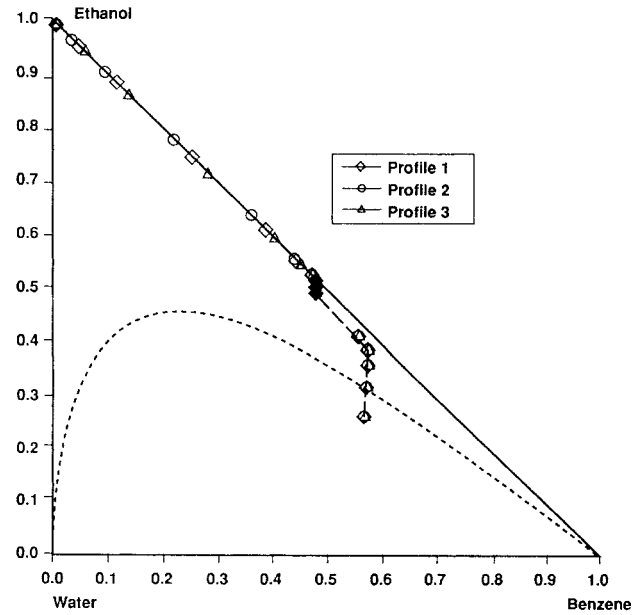

Figure 14. Three different steady-state composition profiles reported in Figures 13a, 13b, and 13c, superimposed on the liquid-liquid-vapor envelope.

Both sets of calculations were carried out using the parameters reported by Prausnitz et al. (1980).

lated using the parameters reported by Prausnitz et al. (1980). From this figure, we see that for all three steady-state solutions the decanter exhibits a liquid-liquid-phase separation; otherwise, every tray in the column is homogeneous. This figure also shows that the three solutions have near-identical shape on a composition triangle, even though the compositions on the trays may vary widely from solution to solution (see Figure 13). Moreover, the transients shown in Figure 12 correspond to the tray compositions "sliding" along a composition profile of almost fixed shape, like beads on an abacus. Figure 15 shows how the steep front of the steady-state temperature profile moves down into the column for the three different steady-state solutions. Thus, for control purposes, it is important to know which steady state the column is actually operating at so that thermocouples can be placed on those trays with the highest sensitivity.

Different values of the reflux ratio, as defined in Figure 11, were also explored. If we associate the different stationary points on the transients with different steady-state solutions (which is justified by previous arguments), then a multiplicity region still exists over a small range of reflux ratios. This range is much smaller than the corresponding range predicted for this system using the parameters reported by Gmehling and Onken (1977a) (Figure 9). However, in all the examples considered with the Prausnitz et al. parameters, the system always drifted towards the lower branch, stable, steady-state conditions corresponding to the profiles reported in Figure 13c. This contrasts with the system behavior predicted using the Gmehling and Onken parameters. For this last case, both the upper and lower branches of steady-state solutions in Figure 9 were dynamically stable for a wide range of initial conditions, and it was possible only to get from one branch to the other by perturbing the system, as demonstrated in Figure 7. Note in Figure 12 that the time spent visiting the two "unstable" or "intermediate" steady states is usually quite large, e.g., 10 hours or more. The system behaves so sluggishly that the entire transient lasts for 24 hours or more.

We therefore see that, when the column is simulated using the Prausnitz et al. UNIQUAC parameters, the transient passes close to two unstable steady states before reaching the final stable node. These unstable steady states must be saddles, and this strongly suggests the presence of other stable and unstable steady states elsewhere in the solution space. This is completely consistent with recent work by Kovach and Seider (1987) who found five steady states for this column using a homotopy continuation method. Therefore, our dynamic simulations verify their bifurcation diagram, and their bifuctation diagram verifies our dynamic simulation.

In an attempt to explain the path from the initial condition via the various steady states to the final stable solution (as shown in Figure 12), we calculated the total energy of the liquid holdup in the system (including reboiler, condenser, and decanter) at each instant of time. This is readily calculated from Eq. 2. In all cases, we found that oscillations in the composition transients were accompanied by corresponding oscillations in the total system energy. As far as we can distinguish, the maxima and the minima in the total system energy response occur at the same time as the visits to the intermediate steady states. For example, for the case considered above with $R = 23.78$ (which led to Figure 12), the total system energy response is shown in Figure 16. The system moves from the initial point to the initial steady state (shown in Figure 13a) at around 300 minutes, which corresponds to the first energy minimum in Figure 16. Then the system moves to the second steady state (shown in Figure 13b), which corresponds to the energy maximum in Figure 16. Finally, the system settles down to the stable solution shown in Figure 13c, which is an absolute minimum in the total system energy.

When the transients are close to an intermediate steady state, the tray temperatures, pressures and compositions are all locally stationary with respect to time, as shown in Figure 12. Thus, the total system energy, $E(T_1, \ldots, T_{N+1}, P_1, \ldots, P_{N+1}, x_{i,1}, \ldots, x_{i,N+1})$, will also be locally stationary with respect to time. This explains the correspondence between the maxima and minima in Figures 12 and 16. Moreover, when the tray temperatures are high, the holdups are also high and the total system energy exhibits a maximum. Thus, the column temperatures, holdup and total energy act in concert.

Although we are unable to prove any other formal correspondence between the state space response of the system (i.e., temporal variation of the tray compositions, temperature, holdups,

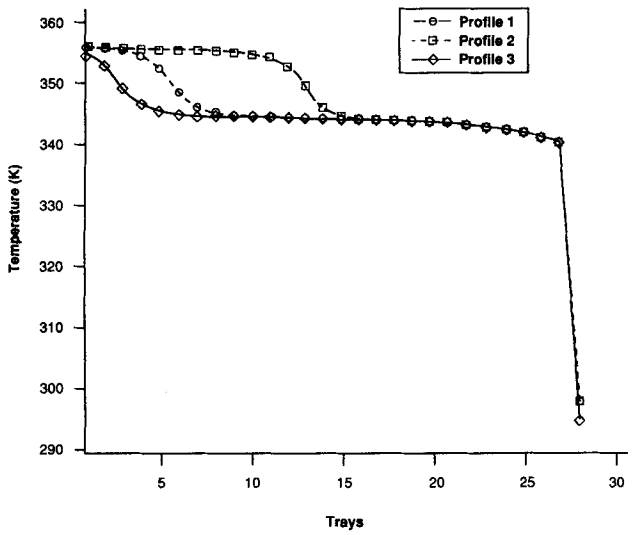

Figure 15. Three different temperature profiles that correspond to the composition profiles reported in Figures 13a, 13b, and 13c.

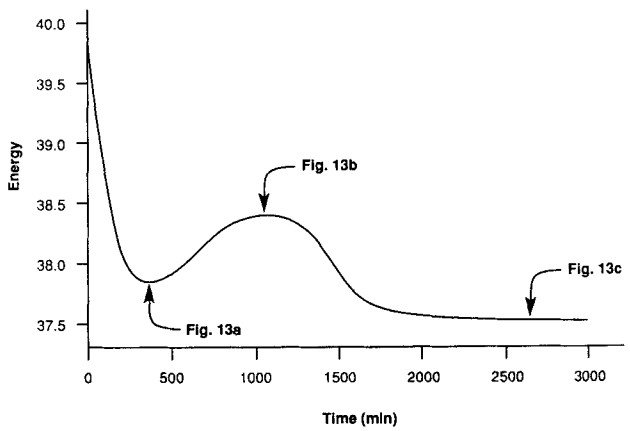

Figure 16. Evolution of the total energy of the column for $R = 23.78$.

etc.) and the response of the total system energy (which is a scalar function), the initial results presented here suggest that the total system energy is either related to or is itself a scalar potential for the process. Identification of such potentials often help to produce intuitive insight into the complex behavior of nonlinear systems, as in the case of simple distillation, for which the temperature acts as a scalar potential (see Van Dongen and Doherty, 1984; Doherty, 1985). Thus, we consider it worthwhile mentioning these results as a pointer for continued analysis.

Parametric Sensitivity

A great number of results and observations available in the literature, as well as from our simulations, can be used to show the very high sensitivity of these heterogeneous systems. Pham, Ryan and Doherty (1989) found that, with a small variation of benzene mole fraction in the bottom of the column, the composition profiles in the stripping section change tremendously. As already mentioned in the introduction, Kovach and Seider (1987) found that a dramatic change in the composition profile occurs as the aqueous reflux ratio is increased by just 0.1%—from 0.1238223 to 0.1239933.

To demonstrate further the high sensitivity of these systems, we show now the following example. In the previous case, reported in Figure 12 with the reflux ratio equal to 23.78, we changed the pressure drop across the vapor line (from the top tray to the condenser) by just 10%—from 0.10 to 0.11 atm—leaving all the other data and specifications exactly the same. Figure 17 shows that, with this very small pressure variation in the column, the overhead vapor composition moves outside the heterogeneous region and the column fails to operate correctly. Such loss of interface in the decanter would cause the entire sequence to shut down. However, the transient is very slow and the phenomenon needs a long time to completely develop its effects. For example, the evolution reported in Figure 17 requires 1,300 minutes of response time.

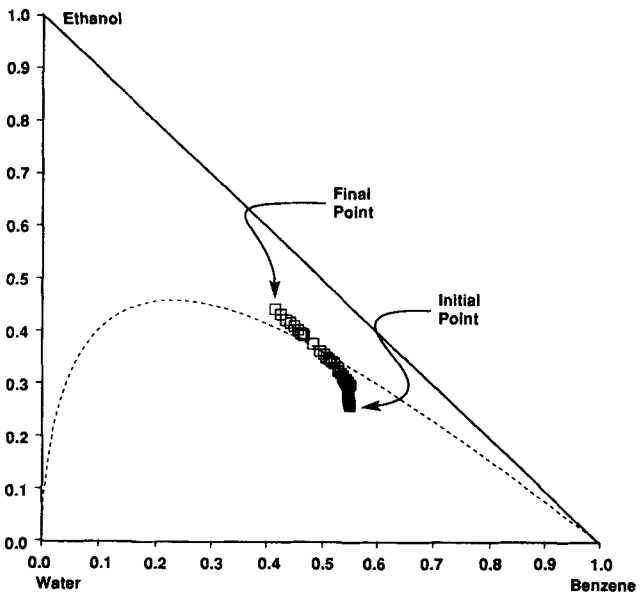

Figure 17. Dramatic change of the overhead vapor composition caused by changing the pressure drop across the vapor line in the top of the column by 10% (from 0.1 to 0.11 atm).

Alternatively, if the condenser-decanter system is vented to the atmosphere, small changes in atmospheric pressure will have the same disastrous effects. As a matter of fact, the same result shown in Figure 17 was obtained by maintaining the original pressure drop in the overhead vapor line (e.g., 0.1 atm) but with an increase of 1% in the barometric pressure (e.g., 1.01 atm instead of 1.0 atm assigned in the previous example).

Furthermore, calculations with a smaller pressure drop (0.09 atm) across the vapor line, were also performed. In this case, the overhead vapor composition does not move outside of the heterogeneous region and the system shows more robust behavior.

Conclusions

Extensive dynamic simulations for a variety of column configurations, operating conditions, and phase equilibrium model parameters have been carried out for the heterogeneous distillation of ethanol, water and benzene. Our results are in general agreement with prior work which shows that this class of separations can be expected to exhibit multiple steady states, complex dynamic behavior, and parametric sensitivity to small changes in operating conditions. Our specific conclusions are summarized as follows:

- Changing the UNIQUAC parameters from the Gmehling and Onken values to the Prausnitz et al. values does not eliminate multiple steady states. However, the shapes of the composition profiles on a triangular diagram are changed. (Compare Figures 10a and 14.) Moreover, for the Prausnitz et al. values, none of the trays inside the column had two liquid phases while as many as 60% of the trays had two liquid phases for the Gmehling and Onken parameters (1977a). (See profile 3 of Figure 10a.)
- Switching off the phase stability test for the trays but not the decanter and performing *only* liquid-vapor equilibrium calculations on the trays for the Gmehling and Onken parameters do not eliminate the multiple steady states. (See Figure 10b.)
- Removing the condenser/decanter feedback system from the model and replacing it by a second feed stream with constant flow rate, composition, and temperature do not eliminate multiple steady states. The state of the second feed stream is taken to be in the general vicinity of where it would be if the decanter were present. Thus, the system still "knows" that a decanter of some sort is present.
- Our dynamic simulations using the Prausnitz et al. UNIQUAC parameters produce transients that "visit" two saddles before settling down at a stable node. Such a set of steady states almost certainly means that there are more steady states elsewhere in the solution space. These dynamic results are consistent with Kovach and Seider's (1987) bifurcation diagrams which show the existence of five steady states for this column. The transients using the Gmehling and Onken parameters are quite different and show no indication of more than three steady states.
- The system shows parametric sensitivity with respect to small changes in column pressure. For systems vented to the atmosphere, small increases in the barometric pressure lead to loss of interface in the decanter over a 24-hour period. If small pressure variations of this sort are left uncontrolled long enough, the entire separation will fail. Small decreases in the barometric pressure do not have such a disastrous effect.

From the results of this and prior research, we conclude that the presence of multiple steady states in heterogeneous distilla-

tions is robust to a variety of manipulations. They clearly do not depend on the trays having multiple liquid phases nor on the detailed behavior of the condenser/decanter system which can actually be eliminated and replaced by a second feed stream with a constant state. Moreover, they occur for both constant molar overflow (Magnussen et al., 1979) and nonconstant molar overflow models (Prokopakis and Seider, 1983a,b; Venkataraman and Lucia, 1988; and this article). Although we are beginning to put together a picture of what does not eliminate multiple steady states, we still do not know what causes them. While it is known that multiple steady states cannot occur in nonideal homogeneous binary distillation (Rosenbrock, 1960, 1962; Doherty and Perkins, 1982, Sridhar and Lucia, 1989), it is still not known whether this is true for binary heterogeneous distillation.

Acknowledgment

This project was supported partially by the Department of Energy (Grant No. DE-FG02-85ER13329) and by the National Science Foundation through the Cornell National Supercomputer Facility.

Notation

C = number of components
c_{N+1} = liquid concentration in the decanter, kmol/m^3
D_d = decanter diameter, m
E_n = internal energy for liquid holdup on tray n, kJ
$F_{i,n}$ = feed flow rate of component i to tray n, kmol/min
g = acceleration due to gravity, m/s^2
H_n^F = molar enthalpy of feed to tray n, kJ/kmol
H_n^L = molar enthalpy of liquid leaving tray n, kJ/kmol
H_n^V = molar enthalpy of vapor leaving tray n, kJ/kmol
h_1 = liquid height corresponding to phase 1 in the decanter, see Figure 3, m
h_2 = liquid height corresponding to phase 2 in the decanter, see Figure 3, m
h_3 = decanter geometric characteristic defined in Figure 3, m
$K_{i,n}$ = liquid-vapor equilibrium coefficient for species i on tray n
L_n = liquid flowrate from tray n, kmol/min
$M_{i,n}$ = liquid holdup of component i on tray n, kmol
M_n^* = holdup reference value on tray n defined by Eq. 3, kmol
N = total number of equilibrium stages in the column
$N+1$ = last stage in the column (condenser-decanter)
P_n = pressure on tray n, atm
Q_n = thermal duty to tray n, kJ/min
R = reflux ratio
s_a = longitudinal section area of the decanter, m^2
s_d = downcomer cross section area of the decanter, m^2
t = time, min
T_n = temperature on tray, n, K
U_n = liquid sidestream from tray n, kmol/min
V_n = vapor flowrate from tray n, kmol/min
W_n = vapor sidestream from tray n, kmol/min
$x_{i,n}$ = liquid mole fraction of species i on tray n
$y_{i,n}$ = vapor mole fraction of species i on tray n
α_n = molar ratio between the amount of phase 1 and the total liquid phase on tray n
$\gamma_{i,n}$ = activity coefficient of species i on tray n
ΔP_n = pressure drop across tray n, atm
ρ = liquid density, kg/m^3
τ_n^l = liquid time constant on tray n, min
τ_n^v = vapor time constant on tray n, min

Subscripts

i = species index
n = tray index

Superscripts

F = feed
L = liquid
sat = saturated
V = vapor
o = overall liquid phase
1 = first liquid phase
2 = second liquid phase

Literature Cited

Bancroft, W. D., and S. S. Hubard, "A New Method for Determining Dineric Distribution," *J. Amer. Chem. Soc.*, **64**, 347 (1942).

Boston, J. F., H. I. Britt, S. Jirapongpham, and V. B. Shah, "An Advanced System for the Simulation of Batch Distillation Operations," *Foundations of Computer Aided Chemical Process Design*, Eng. Foundation, New York (1981).

Buzzi Ferraris, G., and M. Morbidelli, "Distillation Model for Two Partially Immiscible Liquids," *AIChE J.*, **27**, 881 (1981).

Doherty, M. F., "The Presynthesis Problem for Homogeneous Azeotropic Distillation has a Unique Explicit Solution," *Chem. Eng. Sci.*, **40**, 1885 (1985).

Doherty, M. F., and J. D. Perkins, "On the Dynamics of Distillation Processes: IV. Uniqueness and Stability of the Steady State in Homogeneous Continuous Distillations," *Chem. Eng. Sci.*, **37**, 381 (1982).

Eisenstat, S. C., M. C. Gursky, M. H. Schultz, and A. H. Sherman, "Yale Sparse Matrix Package: I and II," Reports Nos. 112 and 114, Dept. of Computer Sciences, Yale University (1977).

Feng, A., C. D. Holland, and S. E. Gallun, "Development and Comparison of a Generalized Semi-Implicit Runge-Kutta Method with Gear's Method for System of Coupled Differential and Algebraic Equations," *Comp. & Chem. Eng.*, **8**, 51 (1984).

Gear, C. W., *Numerical Initial Value Problems in Ordinary Differential Equations*, Prentice Hall, Englewood Cliffs, NJ (1971).

Glitsch & Co., *Ballast Tray Design Manual*, Dallas, TX (1974).

Gmehling, J., and U. Onken, *Vapor-Liquid Equilibrium Data Collection*, DECHEMA, Chemistry Data Series, **I**, Part 1, Verlag and Druckerei Friedrick Bishoff, Frankfurt (1977a).

———, *Vapor-Liquid Equilibrium Data Collection*, DECHEMA, Chemistry Data Series, **I**, Part 2a, Verlag and Druckerei Friedrick Bishoff, Frankfurt (1977b).

Hindmarsh, A. C., *ODEPACK: A Systemized Collection of ODE Solvers*, Lawrence Livermore National Laboratory, Livermore, CA (1983).

Luyben, W. L., *Process Modeling, Simulation, and Control for Chemical Engineerings*, p. 76, McGraw Hill, New York (1973).

Kovach III, J. W., and W. D. Seider, "Heterogeneous Azeotropic Distillation: Experimental and Simulation Results," *AIChE J.*, **33**, 1300 (1987).

———, "Heterogeneous Azeotropic Distillation Homotopy-Continuation Methods," *Comp. & Chem. Eng.*, **11**, 593 (1987).

Magnussen, T. M., L. Michelsen, and A. Fredenslund, "Azeotropic Distillation Using UNIFAC," *Inst. Chem. E. Symp. Ser.*, **56**, pp. 4.2/1–4.2/19, Int. Symp. on Distillation, ICE, Rugby, Warwickshire, England (1979).

Norman, W. S., "The Dehydration of Ethanol by Azeotropic Distillation, Vapour-Liquid Equilibrium Data for the System Ethanol-Benzene-Water," *Trans. Inst. Chem. Eng.*, **23**, 66 (1945).

Nutter & Co., *Float Valve Design Manual*, Tulsa, OK (1976).

Perry, J. H., C. H. Chilton, and S. D. Kirkpatrick, *Chemical Engineers' Handbook*, 4th ed., McGraw-Hill, New York (1969).

Pham, N. H., R. J. Ryan, and M. F. Doherty, "Design and Minimum Reflux for Heterogeneous Axeotropic Distillation Columns," *AIChE J.*, **35**, 1585 (1989).

Prausnitz, J. M., T. F. Anderson, E. A. Grens, C. A. Eckert, R. Hsieh, and J. P. O'Connell, *Computer Calculations for Multicomponent Vapor-Liquid and Liquid-Liquid Equilibria*, Prentice Hall, Englewood Cliffs, NJ (1980).

Prokopakis, G. J., and W. D. Seider,"Feasible Specifications in Azeotropic Distillation," *AIChE J.*, **29**, 49 (1983a).

———, "Dynamic Simulation of Azeotropic Distillation," *AIChE J.*, **29**, 1017 (1983b).

Ranzi, E., M. Rovaglio, S. Pierucci, G. Bussani, and T. Faravelli, "Dinamica degli Impianti Chimici: Apparecchiature di Equilibrio Liquido-Vapore," *Ing. Chim. Ital.*, **21**(7–8), 29 (1985).

Ranzi, E., M. Rovaglio, G. Biardi, R. Binda, and P. Rizzetto, "Multicomponent Distillation Column Under Transient Conditions. II.

Comparison among Different Modelling Schemes," *Ing. Chim. Ital.*, **22**(5–6), 3 (1986).
Rosenbrock, H. H., "A Theorem of 'Dynamic Conservation' For Distillation," *Trans. Instn. Chem. Engrs.*, **38**, 279 (1960).
———, "A Lyapunov Function with Applications to Some Nonlinear Physical Systems," *Automatica*, **1**, 31 (1962).
Rovaglio, M., G. Biardi, E. Ranzi, R. Binda, and P. Rizzetto, "Multicomponent Distillation Column Under Transient Conditions: I. Modelling Approach," *Ing. Chim. Ital.*, **22**(7–8), 3 (1986).
Ryan, P. J., PhD Diss., University of Massachusetts (1989).
Ryan, P. J., and M. F. Doherty, "Design/Optimization of Ternary Heterogeneous Azeotropic Distillation Sequences," *AIChE J.*, **35**, 1592 (1989).
Shewchuk, C. F., PhD Diss., Appendix A1, University of Cambridge, England (1974).
Sridhar, L. N., and A. Lucia, "Analysis and Algorithms for Multistage Separation Processes," *I & EC Res.*, **28**, 793 (1989).
Stephanopoulos, G., *Chemical Process Control: An Introduction to Theory and Practice*, p. 61, Prentice Hall, Englewood Clifts, NJ (1984).
Treybal, R. E., *Mass Transfer Operation*, McGraw Hill, New York (1980).
Van Dongen, D. B., and M. F. Doherty, "On the Dynamic of Distillation Processes: V. The Topology of the Boiling Temperature Surface and Its Relation to Azeotropic Distillation, *Chem. Eng. Sci.*, **39**, 883 (1984).
Venkataraman, S., and A. Lucia, "Solving Distillation Problems by Newton-Like Methods," *Comput. Chem. Eng.*, **12**, 55 (1988).

Manuscript received May 12, 1989, and revision received Nov. 8, 1989.